Synthesis and Crystal and Molecular Structures of Diisopropyl N,N-Diethylcarbamylmethylenephosphonate Samarium Nitrate and Erbium Nitrate Complexes

S. M. BOWEN, E. N. DUESLER and R. T. PAINE*

Department of Chemistry, University of New Mexico, Albuquerque, N.M. 87131, U.S.A.

Received January 11, 1982

Bis[diisopropylN,N-diethylcarbamylmethylenephosphonate] samarium(III) nitrate, $Sm[(i\text{-}C_3H_7O)_2P(O)CH_2C(O)N(C_2H_5)_2]_2(NO_3)_3$ 3 and bis[diisopropyl N,N-diethylcarbamylmethylenephosphonate]-erbium(III) nitrate monohydrate, $Er[(i\text{-}C_3H_7O)_2P(O)CH_2C(O)N(C_2H_5)_2]_2(NO_3)\cdot(H_2O)$ 4 have been prepared from the combination of an ethanolic solution of $Sm(NO_3)_3\cdot 5H_2O$ or $Er(NO_3)_3\cdot 5H_2O$ with phosphonate ligand. The resulting complexes were isolated and characterized by infrared and ^1H, $^{13}C\{^1H\}$ and $^{31}P\{^1H\}$ NMR spectroscopies. In addition, single crystal X-ray analyses of 3 and 4 have been completed. The structure of 3 was determined at −17 °C from 7634 independent reflections obtained with a computer automated diffractometer. The complex crystallizes in the monoclinic space group C2/c with a = 25.672(10) Å, b = 11.431(5) Å, c = 18.731(5) Å, β = 133.73(2)°, Z = 4, V = 3971.5 Å^3 and ρ_{calcd} = 1.50 g cm^{-3}. The structure was solved with standard heavy atom methods and blocked least squares refinement of the structure converged with R_F = 5.6% and R_{wF} = 5.7%. The crystal contains monomeric units of 3 which have crystallographic C_2 symmetry. The samarium atom is bonded to both carbonyl and phosphoryl oxygen atoms of two phosphonate ligands and the oxygen atoms of three bidentate nitrate ions. The overall coordination number of the samarium atom is ten. Several important bond distances include Sm–O (carbonyl) 2.433(2) Å, Sm–O (phosphoryl) 2.418(3) Å, Sm–O (nitrate)$_{avg}$ 2.589(5) Å, P–O (phosphoryl) 1.480(2) Å and C–O (carbonyl) 1.261(3) Å. The structure of 4 was determined at 25 °C from 8432 independent reflections. The compound crystallizes in the triclinic space group $P\bar{1}$ with a = 11.590(2) Å, b = 12.321(2) Å, c = 14.840(4) Å, α = 97.40(2)°, β = 91.85(2)°, γ = 95.17(1)°, Z = 2, V = 2090.9 Å^3 and ρ_{calcd} = 1.48 g cm^{-3}. The structure was solved by standard heavy atom methods and final discrepancy indices R_F = 7.7% and R_{wF} = 7.6% were obtained. The erbium atom is bonded to the phosphoryl oxygen atoms of two phosphonate ligands, the oxygen atoms of three bidentate nitrate ions and the oxygen atom of a water molecule. The carbonyl oxygen atoms are hydrogen bonded to the hydrogen atoms of the coordinated water and the erbium atom coordination number is nine. Several important bond distances include Er–O (phosphoryl)$_{avg}$ 2.275(6) Å, Er–O (nitrate)$_{avg}$ 2.435(8) Å, Er–O (water) 2.302(7) Å, P–O (phosphoryl) 1.479(6) and 1.452(7) Å and C–O (carbonyl) 1.240(11) and 1.239(11) Å.

Introduction

Trivalent lanthanide and actinide ions are efficiently extracted from acidic aqueous solutions into hydrocarbon solvents containing carbamylmethylenephosphonate (CMP) ligands, $(RO)_2P(O)CH_2C(O)NR'_2$ [1]. Siddall [2, 3] first studied the extraction mechanism, and based upon equilibrium distribution measurements, it was concluded that tris bidentate chelate complexes, $M(CMP)_3^{3+}$, were formed in the organic phase during the extraction process. Subsequently, the extraction chemistry has been reexamined by several investigators and similar results have been reported [1, 4–7]. In an attempt to verify the stoichiometry of the proposed solution species, Stewart and Siddall [8] isolated several solid lanthanide–CMP complexes from aqueous ethanol solutions. Compositions corresponding to bis-ligand complexes, $M(CMP)_2(NO_3)_3$ (M = La–Gd) and $M(CMP)_2(NO_3)_3\cdot H_2O$ (M = Tb–Lu), were deduced from elemental analyses, and infrared spectra were interpreted in favor of bidentate ligand chelation with the lanthanide ions. Horwitz and coworkers [9, 10] have recently reinvestigated the extraction chemistry of dihexyl N,N-diethylcarbamylmethylenephosphonate (DHDECMP) with several lanthanide and actinide ions, and they have concluded that monodentate tris chelates are formed

*Author to whom correspondence should be addressed.

0020-1693/82/0000-0000/$02.75

in the organic phase. In addition, they have suggested that the monodentate coordination occurs through metal–phosphoryl oxygen atom interactions and that the amide group functions as an internal buffer.

As part of a study of the coordination characteristics of CMP ligands, we have reported syntheses and crystal and molecular structures for $[Hg((EtO)_2P(O)CHC(O)NEt_2)NO_3]_2$ [11] *1* and $Th[(EtO)_2P(O)CH_2C(O)NEt_2]_2(NO_3)_4$ [12] *2*. In *1*, the CMP ligands are deprotonated at the methylene carbon atom spanning the phosphoryl and carbonyl groups. Each mercury atom in the dimeric molecule is bonded to the methine carbon atom of one deprotonated CMP ligand and to the phosphoryl and carbonyl oxygen atoms of the second deprotonated CMP ligand. In *2*, neutral CMP ligands bond in a bidentate chelate mode with the central thorium atom. These interesting structures and the reported discrepancies in solid state and solution structures for lanthanide–CMP complexes led us to reinvestigate this important chemistry. We report here the synthesis, spectroscopic characterization and single crystal X-ray analyses of Sm(III) and Er(III) complexes with $(i\text{-}C_3H_7O)_2P(O)CH_2C(O)N(C_2H_5)_2$.

Experimental

General Information

The $(i\text{-}C_3H_7O)_2P(O)CH_2C(O)N(C_2H_5)_2$ (Di-PDECMP) was prepared by literature methods [2]. The $Sm(NO_3)_3\cdot 5H_2O$ and $Er(NO_3)_3\cdot 5H_2O$ were purchased from Ventron Corp. Infrared spectra were recorded on a Nicolet Model 6000 FT-IR spectrometer by using KBr pellets and 0.05 *M* benzene solutions contained in a solution cell fitted with sealed NaCl windows. NMR spectra were recorded on a Varian XL-100 NMR spectrometer operated at 40.5 MHz (^{31}P) and a Varian FT-80 NMR spectrometer operated at 20.0 MHz (^{13}C) and 80.0 MHz (^1H). Samples were contained in 5 mm tubes. On the XL-100 spectrometer, the 5 mm tubes were rigidly suspended in a 12 mm tube containing a deuterated lock solvent. On the FT-80 spectrometer, the 5 mm tubes contained an internal deuterium lock solvent. Spectral standards were 85% H_3PO_4 (^{31}P) and $(CH_3)_4Si$ (^{13}C and ^1H).

Preparation of the Complexes

Typically 21 mmol of $(i\text{-}C_3H_7O)_2P(O)CH_2C(O)N(C_2H_5)_2$ was added to 7 mmol of $Sm(NO_3)_3\cdot 5H_2O$ or $Er(NO_3)_3\cdot 5H_2O$ dissolved in 40 ml EtOH. The mixtures were placed in sealed plastic bottles and shaken overnight. The EtOH solutions were allowed to slowly evaporate and crystalline solids were isolated after several days. The solids were washed with hexane and dried *in vacuo*. The solids were found to have the compositions $Sm[(i\text{-}C_3H_7O)_2P(O)CH_2C(O)N(C_2H_5)_2]_2(NO_3)_3$ *3* and $Er[(i\text{-}C_3H_7O)_2P(O)CH_2C(O)N(C_2H_5)_2]_2(NO_3)_3(H_2O)$ *4*. *Anal.* *3*, Calcd. for $SmC_{24}O_{17}N_5P_2H_{52}$: C, 32.2; H, 5.86; O, 30.4; N, 7.82; P, 6.92; Sm, 16.8. Found: C, 32.4; H, 5.99; O, 30.3; N, 7.78; P, 7.03; Sm, 16.5. *Anal.* *4*, Calcd for $ErC_{24}O_{18}N_5P_2H_{54}$: C, 31.0; H, 5.85; O, 31.0; N, 7.53; P, 6.66; Er, 18.0. Found: C, 31.5; H, 5.86; O, 29.7; N, 7.53; P, 6.84; Er, 18.1. Infrared spectra (cm^{-1}) (KBr pellet) *3*: 1617 (ν_{CO}, m), 1593 (ν_{CO}, m), 1206 (ν_{PO}, m), 1007 (ν_{POC}, s); *4*: 1621 (ν_{CO}, m), 1207 (ν_{PO}, m), 1012 (ν_{POC}, s); (benzene solution) *3*: 1610(s), 1213(m), 1005(s); *4*: 1615(s), 1212(s), 1005(s). NMR spectra ($CHCl_3$ solvent, 27 °C) *3*: $^{31}P\{^1H\}$ δ 21.12; $^{13}C\{^1H\}$ δ 166.0 ($^2J_{PC(2)}$ = 5.9 Hz), 73.9 ($^2J_{PC(7)}$ = 6.9 Hz), 43.4; 41.7, 31.6 ($^1J_{PC(1)}$ = 140.4 Hz), 23.5, 13.8, 12.1; ^1H δ 4.98, 3.75 ($^2J_{PH}$ = 22.6 Hz), 3.40, 1.31, 1.04; *4*: $^{31}P\{^1H\}$ not observed; $^{13}C\{^1H\}$ δ 129, 65.2 ($^2J_{PC(7)}$ = 4.2 Hz), 41.7, 38.5, 19.1, 14.0, 13.0. The crystalline solids are soluble in water, ethanol, chloroform and benzene.

Crystal Structure Determinations

Suitable crystals were obtained from the ethanol evaporates: *3* (0.68 mm × 0.49 mm × 0.43 mm) and *4* (0.34 mm × 0.28 mm × 0.47 mm). The crystals were glued to the end of glass fibers. The crystals were centered on a Syntex P3/F automated diffractometer and the determinations of the crystal classes, orientation matrices and unit cell dimensions were performed in a standard manner [14]. Data were collected at −17 °C for *3* and 25 °C for *4* in the $\theta-2\theta$ scan mode using Mo-K_α radiation, a scintillation counter and pulse height analyzer. The details of the data collections are summarized in Table I.

Inspection of the data for *3* revealed systematic absences, h + k = 2n + 1 for hkl and l = 2n + 1 for h0l, consistent with the monoclinic space group $C2/c$ or its noncentric counterpart Cc. For *4*, the collected data were consistent with the assignment of the triclinic space group $P\bar{1}$ or P1. Corrections for absorption were made empirically based upon ψ scans. Redundant and equivalent reflection data were averaged and converted to unscaled $|F_o|$ values after corrections for Lorentz and polarization effects.

Solution and Refinement of the Structures

All calculations were performed on a R3/SHELXTL structure determination package [14]. Anomalous dispersion terms were included for all atoms where Z > 2. Least-squares refinement in this package uses a blocked cascade algorithm with full matrix blocks of 103 parameters [15].

The initial solution and refinement of the structure of *3* were based on 6730 reflections with $F \geq 4\sigma(F)$ and $\sin\theta \leq 0.57$ [16]. The samarium

TABLE I. Experimental Data for the X-Ray Diffraction Study of $Sm[(i\text{-}C_3H_7O)_2P(O)CH_2C(O)N(C_2H_5)_2]_2(NO_3)_3$ *3*, and $Er[(i\text{-}C_3H_7O)_2P(O)CH_2C(O)N(C_2H_5)_2]_2(NO_3)_3 \cdot H_2O$, *4*.

	3	*4*
Crystal System	Monoclinic	Triclinic
Space Group	*C2/c*	*P1*
a, Å	25.672(10)	11.590(2)
b, Å	11.431(5)	12.321(2)
c, Å	18.731(5)	14.840(4)
α, deg		97.40(2)
β, deg	133.73(2)	91.85(2)
γ, deg		95.17(1)
V Å^3	3971.5	2090.9
Z	4	2
F(000)	1836	950
mol. wt.	895.1	929.9
ρ(calcd), g cm^{-3}	1.50	1.48
ρ(obsd), g cm^{-3}	1.47	1.47
diffractometer	Syntex P 3/F	Syntex P 3/F
radiation	MoK_α ($\bar{\lambda}$ = 0.71069 Å)	MoK_α ($\bar{\lambda}$ = 0.71069 Å)
temperature	−17 °C (+2 °C)	25 °C
monochromator	highly oriented graphite crystal	highly oriented graphite crystal
reflections measured	±h, +k, −l	±h, −k, ±l
2θ range	1°−75°	1°−63°
scan type	$\theta-2\theta$	$\theta-2\theta$
scan speed	5.86−29.3°/min	3.91−29.3°/min
scan range	from $[2\theta(K\alpha_1) - 1.0]°$ to $[2\theta(K\alpha_2) + 1.0]°$	from $[2\theta(K\alpha_1) - 1.0]°$ to $[2\theta(K\alpha_2) + 1.0]°$
unique reflections	10,339	13,989
	$2\sigma(I) \leqslant 7634$	$3\sigma(I) \leqslant 8432$
reflections with weights = $1/(\sigma(F)^2 + gF^2)$	g = 0.001	0.0025
extinction parameter, $F = F_o[1 - (x\lvert F_o\rvert^2 \cdot 10^{-4}/\sin\theta)]$: x = $[\Sigma w(\lvert F_o\rvert - \lvert F_c\rvert)^2/(m-n)]^{1/2}$	0.00016(4)	0.0007(2)
	1.154	1.074

atom was located on the crystallographic C2 axis at 0, 0.15, 0.25 using Patterson methods for the space group *C2/c*, and subsequent Fourier syntheses revealed the locations of all remaining nonhydrogen atoms. Refinement of the positional and individual isotropic thermal parameters of the nonhydrogen atoms by means of a block diagonal least-squares procedure gave convergence at R_F = 7.4%. Refinement by a block diagonalized least-squares procedure using the weighting scheme $w = [\sigma^2(F_o) + gF^2]^{-1}$, where g = 0.001, and an isotropic extinction parameter, x = 0.00016(4) [17], gave convergence at R_F = 5.4%. The hydrogen atom positions were idealized with appropriate bond angles and distances. A final least squares refinement with no restrictions on sin θ and with 7634 reflections gave R_F = 5.6% and R_{wF} = 5.2%. A final difference map showed the two highest peaks (2.5 and 1.1 eÅ^{-3}) to be ≤0.75 Å from the Sm atom. The remaining peaks were ≤1.0 eÅ^{-3}. A table of observed and calculated structure factor amplitudes is available (Table S-1) [18]. Fractional atomic coordinates and thermal parameters are given in Table II.

The solution and refinement of the structure of *4* were based on 8432 independent reflections with $F \geqslant 3\sigma(F)$. The erbium atom was located using Patterson methods in the space group $P\bar{1}$ and difference Fourier syntheses revealed the locations of all remaining nonhydrogen atoms. A difference map without the methyl carbon atom C(16) indicated two possible sites, C(16) and C(16′) for this atom. Each was given one-half occupancy and U_{iso} varied with the positional parameters. Refinement of the positional and isotropic thermal parameters as described above (x = 0.0007(2)) gave convergence R_F = 10.4%. Individual anisotropic thermal parameters were applied to the nonhydrogen atoms and refinement gave R_F = 8.0%. Earlier difference maps

TABLE II. Fractional Coordinates and Thermal Parameters (A × 10^3) for $Sm[(i\text{-}C_3H_7O)_2P(O)CH_2C(O)N(C_2H_5)_2]_2(NO_3)_3$.

Atom	x/a	y/b	z/c	U_{11}	U_{22}	U_{33}	U_{23}	U_{13}	U_{12}
Sm	0.00000(0)	0.15414(2)	0.25000(0)	23.7(1)	24.9(1)	21.9(1)	0	14.1(1)	0
P(1)	0.13722(4)	0.14118(7)	0.51763(6)	27.1(3)	30.2(4)	23.7(3)	4.4(3)	15.9(3)	1.3(3)
O(1)	0.0754(1)	0.0912(2)	0.4195(2)	29(1)	33(1)	26(1)	3(1)	15(1)	−3(1)
O(2)	0.1209(2)	0.1898(2)	0.5778(2)	49(1)	35(1)	40(1)	0(1)	35(1)	−3(1)
O(3)	0.1993(1)	0.0507(3)	0.5879(2)	37(1)	40(1)	29(1)	7(1)	18(1)	9(1)
O(4)	0.0667(1)	0.3263(2)	0.3516(2)	29(1)	30(1)	25(1)	−1(1)	14(1)	−3(1)
O(5)	0.1383(2)	0.1456(3)	0.3314(2)	49(2)	54(2)	42(1)	10(1)	34(1)	7(1)
O(6)	0.0555(1)	0.2186(3)	0.1863(2)	32(1)	70(2)	36(1)	3(1)	21(1)	0(1)
O(7)	0.0461(2)	−0.0454(3)	0.2597(3)	59(2)	39(1)	58(2)	3(1)	47(2)	7(1)
O(8)	0.0000(0)	−0.2113(5)	0.2500(0)	146(6)	30(2)	133(6)	0	108(6)	0
O(9)	0.1652(2)	0.2042(5)	0.2508(3)	40(2)	157(4)	54(2)	18(3)	35(2)	−4(2)
N(1)	0.1217(2)	0.4632(3)	0.4708(2)	33(1)	32(1)	28(1)	−4(1)	16(1)	−7(1)
N(2)	0.1216(2)	0.1896(4)	0.2569(3)	33(1)	69(2)	36(2)	−5(2)	25(1)	−10(2)
N(3)	0.0000(0)	−0.1036(4)	0.2500(0)	79(4)	28(2)	57(3)	0	52(3)	0
C(1)	0.1759(2)	0.2655(3)	0.5112(2)	23(1)	35(2)	26(1)	1(1)	14(1)	−3(1)
C(2)	0.1181(2)	0.3559(3)	0.4404(2)	27(1)	30(1)	26(1)	−1(1)	17(1)	−7(1)
C(3)	0.1805(2)	0.5071(4)	0.5721(3)	45(2)	44(2)	33(2)	−11(2)	18(2)	−12(2)
C(4)	0.1603(5)	0.5101(8)	0.6308(5)	128(6)	147(7)	66(4)	−57(4)	75(5)	−72(6)
C(5)	0.0635(2)	0.5441(4)	0.3971(3)	42(2)	33(2)	39(2)	−2(2)	19(2)	1(1)
C(6)	−0.0061(3)	0.5224(5)	0.3717(5)	45(2)	61(3)	79(4)	−8(3)	37(3)	5(2)
C(7)	0.0932(3)	0.1184(4)	0.6107(4)	71(3)	43(2)	80(4)	3(2)	66(3)	−1(2)
C(8)	0.0196(3)	0.1587(6)	0.5583(4)	44(2)	143(7)	52(3)	9(4)	33(2)	−5(3)
C(9)	0.1450(3)	0.1383(9)	0.7212(5)	51(3)	230(11)	52(3)	53(5)	33(3)	10(4)
C(10)	0.2172(3)	−0.0349(4)	0.5491(4)	52(2)	47(2)	52(2)	7(2)	32(2)	18(2)
C(11)	0.2970(3)	−0.0377(6)	0.6202(5)	57(3)	86(4)	96(5)	17(4)	57(3)	14(3)
C)12)	0.1843(4)	−0.1468(5)	0.5373(8)	83(5)	44(3)	169(10)	−16(4)	77(6)	−5(3)

Atom	x/a	y/b	z/c	U_{iso}
HC(11)	0.1981	0.2412	0.4884	38
HC(12)	0.2116	0.2996	0.5757	38
HC(31)	0.2216	0.4569	0.6054	58
HC(32)	0.1927	0.5849	0.5687	58
HC(41)	0.2001	0.5394	0.6959	127
HC(42)	0.1485	0.4326	0.6354	127
HC(43)	0.1193	0.5604	0.5984	127
HC(51)	0.0794	0.6223	0.4224	55
HC(52)	0.0538	0.5367	0.3378	55
HC(61)	−0.0417	0.5783	0.3232	81
HC(62)	0.0025	0.5303	0.4302	81
HC(63)	−0.0231	0.4447	0.3456	81
HC(71)	0.0902	0.0366	0.5969	65
HC(81)	0.0005	0.1122	0.5785	94
HC(82)	−0.0107	0.1507	0.4884	94
HC(83)	0.0212	0.2393	0.5741	94
HC(91)	0.1298	0.0933	0.7474	114
HC(92)	0.1454	0.2198	0.7339	114
HC(93)	0.1925	0.1145	0.7522	114
HC(101)	0.1986	−0.0154	0.4852	64
HC(111)	0.3114	−0.0924	0.5977	95
HC(112)	0.3167	−0.0611	0.6840	95
HC(113)	0.3145	0.0388	0.6247	95
HC(121)	0.1952	−0.2038	0.5115	108
HC(122)	0.1330	−0.1376	0.4923	108
HC(123)	0.2032	−0.1726	0.6002	108

The anisotropic temperature factor exponent takes the form: $-2\pi^2(h^2a^{*2}U_{11} + k^2b^{*2}U_{22} + \ldots + 2hka^*b^*U_{12} + \ldots)$

TABLE III. Fractional Coordinates and Thermal Parameters (A × 10^3) for $Er[(i\text{-}C_3H_7O)_2P(O)CH_2C(O)N(C_2H_5)_2(NO_3)_3 \cdot H_2O$.

Atom	x/a	y/b	z/c	U_{11}	U_{22}	U_{33}	U_{23}	U_{13}	U_{12}
Er	0.23853(3)	0.14254(3)	0.28211(2)	41.3(2)	44.0(2)	44.5(2)	10.7(1)	4.6(1)	4.1(1)
P(1)	0.1916(2)	0.1473(2)	0.5267(1)	48(1)	42(1)	45(1)	7(1)	1(1)	5(1)
O(1)	0.2342(5)	0.1593(5)	0.4354(4)	57(3)	62(4)	46(3)	4(3)	4(3)	8(3)
O(2)	0.2032(5)	0.0337(5)	0.5577(4)	57(4)	53(4)	75(4)	21(3)	0(3)	17(3)
O(3)	0.2549(6)	0.2349(5)	0.6018(4)	66(4)	64(4)	53(3)	6(3)	−1(3)	−8(3)
O(4)	0.0330(6)	0.3260(5)	0.4767(4)	106(5)	54(4)	60(4)	28(3)	33(4)	30(4)
N(1)	−0.0500(7)	0.3166(6)	0.6107(5)	74(5)	47(4)	62(4)	14(3)	21(4)	20(4)
C(1)	0.0390(7)	0.1558(6)	0.5359(6)	47(4)	42(4)	64(5)	12(4)	6(4)	6(3)
C(2)	0.0058(7)	0.2726(6)	0.5393(6)	51(4)	36(4)	65(5)	11(4)	12(4)	11(3)
C(3)	−0.0837(9)	0.4299(7)	0.6118(7)	95(7)	44(5)	85(7)	16(5)	31(6)	25(5)
C(4)	−0.2051(12)	0.4303(10)	0.5721(11)	113(11)	64(7)	182(15)	21(8)	6(10)	41(7)
C(5)	−0.0875(11)	0.2610(9)	0.6864(8)	113(9)	64(6)	99(9)	36(6)	63(8)	31(6)
C(6)	−0.0028(16)	0.2880(15)	0.7658(9)	209(19)	173(16)	74(9)	54(10)	10(11)	46(15)
C(7)	0.3142(11)	−0.0155(9)	0.5691(10)	85(8)	61(6)	154(12)	37(7)	−37(8)	13(6)
C(8)	0.2927(18)	−0.1304(14)	0.5360(16)	186(19)	115(14)	300(28)	−32(15)	−107(18)	92(14)
C(9)	0.3605(25)	0.0039(19)	0.6525(18)	391(35)	209(23)	320(31)	−91(21)	−263(28)	201(25)
C(10)	0.3198(10)	0.3363(8)	0.5824(7)	87(7)	61(6)	71(6)	9(5)	−12(5)	−27(5)
C(11)	0.2832(13)	0.4256(10)	0.6488(10)	134(12)	68(8)	134(12)	−15(8)	−5(10)	−20(8)
C(12)	0.4449(12)	0.3205(15)	0.5863(12)	84(9)	163(15)	150(15)	23(12)	4(9)	−31(10)
P(2)	0.2282(2)	0.2662(2)	0.0682(2)	55(1)	61(1)	49(1)	13(1)	12(1)	3(1)
O(5)	0.2556(5)	0.2272(5)	0.1539(4)	56(3)	60(3)	60(4)	23(3)	14(3)	2(3)
O(6)	0.2776(6)	0.2024(6)	−0.0171(5)	82(5)	75(4)	63(4)	6(3)	26(4)	3(4)
O(7)	0.2726(6)	0.3876(5)	0.0651(4)	82(5)	58(4)	65(4)	20(3)	13(3)	−4(3)
O(8)	0.0418(6)	0.3641(6)	0.1661(4)	69(4)	77(4)	59(4)	9(3)	5(3)	21(3)
N(2)	−0.1131(7)	0.2716(8)	0.0873(7)	57(5)	99(7)	94(7)	8(5)	3(5)	16(5)
C(13)	0.0773(8)	0.2444(9)	0.0335(6)	71(6)	94(7)	45(5)	8(5)	0(4)	7(5)
C(14)	−0.0011(8)	0.2979(8)	0.1011(6)	67(6)	75(6)	53(5)	25(4)	4(4)	19(5)
C(15)	−0.1923(12)	0.3232(16)	0.1543(12)	73(8)	204(18)	132(13)	−18(12)	19(8)	43(10)
C(16)	−0.2363(34)	0.4159(42)	0.1324(24)	164(30)	309(46)	106(23)	−58(28)	−30(21)	161(32)
C(16′)	−0.2143(42)	0.2740(35)	0.2277(29)	257(42)	164(33)	173(33)	9(27)	151(32)	40(31)
C(17)	−0.1698(10)	0.1893(11)	0.0108(8)	67(7)	116(10)	85(8)	22(7)	−10(6)	1(7)
C(18)	−0.1927(16)	0.0773(13)	0.0370(12)	174(17)	120(13)	143(15)	18(11)	−66(13)	−17(12)
C(19)	0.3952(11)	0.2187(13)	−0.0476(10)	70(7)	142(12)	106(10)	−2(9)	31(7)	15(8)
C(22)	0.3115(13)	0.4645(10)	0.1460(9)	121(11)	70(7)	105(10)	10(7)	38(8)	−7(7)
C(24)	0.4344(16)	0.4735(16)	0.1537(13)	173(18)	144(16)	168(18)	−16(14)	−12(15)	−53(14)
N(3)	0.0182(7)	0.0162(7)	0.2340(7)	60(5)	80(6)	90(7)	29(5)	−16(5)	−13(4)
O(9)	0.0680(6)	0.0218(6)	0.3118(5)	68(4)	79(5)	84(5)	39(4)	−8(4)	−15(4)
O(10)	0.0712(6)	0.0691(6)	0.1791(5)	76(5)	94(5)	62(4)	23(4)	1(3)	−22(4)
O(11)	−0.0745(8)	−0.0382(10)	0.2161(8)	85(6)	171(10)	141(9)	71(7)	−48(6)	−72(6)
N(4)	0.3193(8)	−0.0694(7)	0.2415(8)	67(5)	52(5)	116(8)	−1(5)	29(5)	17(4)
O(12)	0.3083(7)	−0.0257(6)	0.3211(5)	115(6)	65(4)	84(5)	26(4)	35(5)	40(4)
O(13)	0.2973(9)	−0.0105(8)	0.1825(5)	140(8)	106(6)	64(5)	−4(5)	7(5)	56(6)
O(14)	0.3494(9)	−0.1608(7)	0.2238(8)	124(7)	63(5)	182(10)	−7(5)	56(7)	34(5)
N(5)	0.4484(10)	0.2742(10)	0.3247(9)	96(8)	91(8)	149(11)	59(8)	−44(7)	−29(6)
O(15)	0.3581(7)	0.3162(6)	0.3355(6)	88(5)	76(5)	94(6)	21(4)	−9(4)	−10(4)
O(16)	0.4463(7)	0.1752(8)	0.2922(8)	54(5)	98(7)	214(12)	44(7)	−15(6)	7(5)
O(17)	0.5458(10)	0.3266(11)	0.3398(13)	84(7)	155(11)	383(23)	106(13)	−76(10)	−59(7)
O(18)	0.1067(6)	0.2699(6)	0.3127(4)	87(5)	85(5)	55(4)	24(3)	18(3)	44(4)

Atom	x/a	y/b	z/c	U_{iso}
C(20)	0.4459(36)	0.1094(35)	−0.0514(29)	151(14)
C(20′)	0.4794(30)	0.1700(29)	0.0022(24)	123(10)
C(21)	0.3826(29)	0.2514(30)	−0.1425(23)	117(10)
C(21′)	0.3762(35)	0.1704(36)	−0.1488(27)	142(13)
C(23)	0.2962(45)	0.5770(43)	0.1390(35)	176(19)
C(23′)	0.2378(29)	0.5729(27)	0.1149(22)	103(9)

(continued overleaf)

TABLE III. *(continued)*

Atom	x/a	y/b	z/c	U_{iso}
HO(181)	0.073(8)	0.294(7)	0.274(6)	70
HO(182)	0.081(8)	0.282(7)	0.359(6)	70
HC(11)	0.0154	0.1277	0.5905	50
HC(12)	−0.0008	0.118	0.4842	50
HC(31)	−0.0799	0.4651	0.6736	74
HC(32)	−0.0306	0.4699	0.5769	74
HC(41)	−0.2238	0.5047	0.5733	117
HC(42)	−0.2590	0.3916	0.6073	117
HC(43)	−0.2098	0.3947	0.5104	117
HC(51)	−0.1613	0.2840	0.7046	87
HC(52)	−0.0951	0.1831	0.6678	87
HC(61)	−0.0293	0.2500	0.8149	146
HC(62)	0.0045	0.3658	0.7852	146
HC(63)	0.0712	0.2653	0.7481	146
HC(71)	0.3727	0.0194	0.5353	102
HC(81)	0.3630	−0.1651	0.5419	203
HC(82)	0.2671	−0.1389	0.4731	203
HC(83)	0.2340	−0.1640	0.5704	203
HC(91)	0.4318	−0.0298	0.6556	316
HC(92)	0.3064	−0.0272	0.6920	316
HC(93)	0.3752	0.0816	0.6712	316
HC(101)	0.3039	0.3554	0.5229	77
HC(111)	0.3229	0.4944	0.6384	117
HC(112)	0.3026	0.4115	0.7094	117
HC(113)	0.2010	0.4291	0.6420	117
HC(121)	0.4891	0.3860	0.5735	135
HC(122)	0.4595	0.2599	0.5420	135
HC(123)	0.4673	0.3052	0.6459	135
HC(131)	0.0550	0.1667	0.0244	70
HC(132)	0.0671	0.2736	−0.0229	70
HC(171)	−0.1192	0.1857	−0.0392	93
HC(172)	−0.2420	0.2140	−0.0077	93
HC(181)	−0.2280	0.0284	−0.0141	155
HC(182)	−0.2440	0.0796	0.0865	155
HC(183)	−0.1210	0.0515	0.0554	155
HC(241)	0.4606	0.5238	0.2068	176
HC(242)	0.4656	0.5002	0.1007	176
HC(243)	0.4602	0.4027	0.1590	176

The anisotropic temperature factor exponent takes the form: $-2\pi^2(h^2a^{*2}U_{11} + k^2b^{*2}U_{22} + \ldots + 2hka^*b^*U_{12})$.

and large thermal parameters for the methyl carbon atoms, C(20), C(21) and C(23), indicated that these atoms were disordered over several sites. Each atom was located at two sites [C(20), C(20′); C(21), C(21′); C(23), C(23′)] and given one-half occupancy. Each atom was assigned an isotropic thermal parameter and U_{iso} was allowed to vary. The difference map without C(9) would not resolve the electron density into discrete regions, consequently, no disorder model was used to fix the large thermal motions of C(9). Further least-squares cycles led to an R_F = 8.0%. Hydrogen atom positions were idealized for all carbon atoms with appropriate bond distances and angles. The hydrogen atoms of the bonded water molecule were located by a subsequent difference Fourier synthesis. The water hydrogen atoms were found to be in a position to hydrogen bond with the carbonyl oxygen atom. To test the reliability of these hydrogen atom positions, the hydrogen atoms were allowed to vary in x, y, z for the last 20 cycles of least-squares refinement. The final least-squares refinement gave R_F = 7.7% and R_{wF} = 7.6%. A final difference Fourier synthesis revealed the highest peaks (1.89–1.53 eÅ^{-3}) to be ≤0.86 Å from the Er atom. The remaining peaks were less than 1.05 eÅ^{-3}. The observed and calculated structure factor amplitudes for *4* are available (Table S-3) [18]. The fractional coordinates and thermal parameters are given in Table III.

Results and Discussion

The combination of $(i\text{-}C_3H_7O)_2P(O)CH_2C(O)N(C_2H_5)_2$, DiPDECMP, with $Sm(NO_3)_3 \cdot 5H_2O$ and

$Er(NO_3)_3 \cdot 5H_2O$ in ethanol results in the formation of a yellow crystalline solid *3* and a pink crystalline solid *4* after partial evaporation of the solvent. The compounds are soluble in water, ethanol, chloroform and benzene. Elemental analyses indicate that *3* contains two CMP ligands and three nitrate groups bonded to a samarium ion, and *4* contains two CMP ligands, three nitrate groups, and a water molecule bonded to an erbium ion. The chemistry is consistent with the following equations.

$$2(\text{DiPDECMP}) + Sm(NO_3)_3 \cdot 5H_2O \xrightarrow{\text{ethanol}}$$

$$Sm(\text{DiPDECMP})_2(NO_3)_3 + 5H_2O$$
3

$$2(\text{DiPDECMP}) + Er(NO_3)_3 \cdot 5H_2O \xrightarrow{\text{ethanol}}$$

$$Er(\text{DiPDECMP})_2(NO_3)_3 \cdot H_2O + 4H_2O$$
4

Infrared spectra show bands for *3* at 1617 cm^{-1} and 1593 cm^{-1} (KBr) [19] and 1610 cm^{-1} (benzene) and for *4* at 1621 cm^{-1} (KBr) and 1615 cm^{-1} (benzene) which can be assigned to carbonyl stretches by comparison to ν_{CO} in free DiPDECMP, 1648 cm^{-1}. Bands for *3* at 1206 cm^{-1} (KBr) and 1213 cm^{-1} (benzene) and for *4* at 1207 cm^{-1} (KBr) and 1212 cm^{-1} (benzene) can be assigned to phosphoryl stretches by comparison to ν_{PO} in DiPDECMP, 1253 cm^{-1}. The ν_{CO} and ν_{PO} down-frequency shifts upon complexation suggest that the lanthanide ions interact with both the CMP ligand carbonyl and phosphoryl groups in a bidentate coordination mode.

The ^{31}P, ^{13}C, and ^{1}H NMR spectra of *3* and *4* are of interest. The $^{31}P\{^{1}H\}$ spectrum of *3* in $CHCl_3$ solution shows a singlet 21.1 ppm downfield of H_3PO_4. This resonance is slightly upfield from the free ligand resonance, 22.0 ppm, and from the resonances in two diamagnetic metal complexes, $Th(\text{DiPDECMP})_2(NO_3)_4$ 22.91 ppm [12] and $[Hg(\text{DiPDECMP})(NO_3)]_2$ 27.0 ppm [11]. The $^{13}C\{^{1}H\}$ NMR spectrum of *3* shows resonances at 31.57 ppm ($^{1}J_{PC}$ = 140.4 Hz) and 166.0 ppm ($^{2}J_{PC}$ = 5.9 Hz) which can be assigned to the bridging methylene carbon atom, and the carbonyl carbon atom. These data compare favorably with resonances in DiPDECMP 34.81 ppm ($^{1}J_{PC}$ = 133.6 Hz) and 169.2 ppm ($^{2}J_{PC}$ = 5.7 Hz). In addition, resonances are observed for each of the carbon environments in the Et and i-Pr groups. The ^{1}H NMR spectrum of *3* shows a resonance at 3.75 ppm ($^{2}J_{PH}$ = 22.6 Hz) which can be correlated with a resonance at 2.86 ppm ($^{2}J_{PH}$ = 22.0 Hz) in DiPDECMP, and these resonances can be assigned to the central CH_2 group spanning the PO and CO groups. Although the NMR spectra for *3* are consistent with CMP ligand coordination with the samarium ion, an assignment of the nation with the samarium ion, an assignment of the CMP ligand denticity cannot be made without a detailed analysis of the paramagnetic influences on the chemical shifts for *3* and related lanthanide–CMP complexes [20]. Such a study is in progress. The deleterious influence of the paramagnetic ion Er(III) upon the ^{31}P and ^{1}H NMR spectra of *4* results in heavily broadened lines. The $^{13}C\{^{1}H\}$ spectrum of *4* shows several well resolved resonances for the carbon atoms in the Et and i-Pr groups, and a broad resonance centered at 129 ppm can be tentatively assigned to the ligand carbonyl group. A resonance for the methylene carbon atom was not detected.

The analytical and spectroscopic data indicate that *3* and *4* are identical to the compounds reported earlier by Siddall and Stewart [8]. The data also are consistent with bis-bidentate CMP ligand coordination with Sm(III) and Er(III), but they do not provide an unequivocal structure assignment for the complexes. As a result, single crystal X-ray diffraction analyses have been completed for both complexes. Although it is expected that there may be differences in solid state and solution structures, the solid state structures provide a useful starting point for understanding the nature of the CMP ligand–lanthanide coordination chemistry and the extraction processes.

TABLE IV. Selected Interatomic Distances (Å) for $Sm(\text{DiPDECMP})_2(NO_3)_3$.

Sm–O(1)	2.418(3)
Sm–O(4)	2.433(2)
Sm–O(5)	2.731(4)
Sm–O(6)	2.518(5)
Sm–O(7)	2.518(4)
P(1)–O(1)	1.480(2)
P(1)–O(2)	1.552(5)
P(1)–O(3)	1.562(3)
P(1)–C(1)	1.784(4)
O(2)–C(7)	1.469(10)
O(3)–C(10)	1.468(8)
C(7)–C(8)	1.477(9)
C(7)–C(9)	1.515(9)
C(10)–C(11)	1.484(8)
C(10)–C(12)	1.462(10)
C(1)–C(2)	1.518(4)
C(2)–O(4)	1.261(3)
C(2)–N(1)	1.328(5)
C(3)–N(1)	1.474(4)
C(5)–N(1)	1.463(4)
C(3)–C(4)	1.505(15)
C(5)–C(6)	1.518(10)
N(2)–O(5)	1.248(7)
N(2)–O(6)	1.279(4)
N(2)–O(9)	1.212(8)
N(3)–O(7)	1.257(5)
N(3)–O(8)	1.232(7)

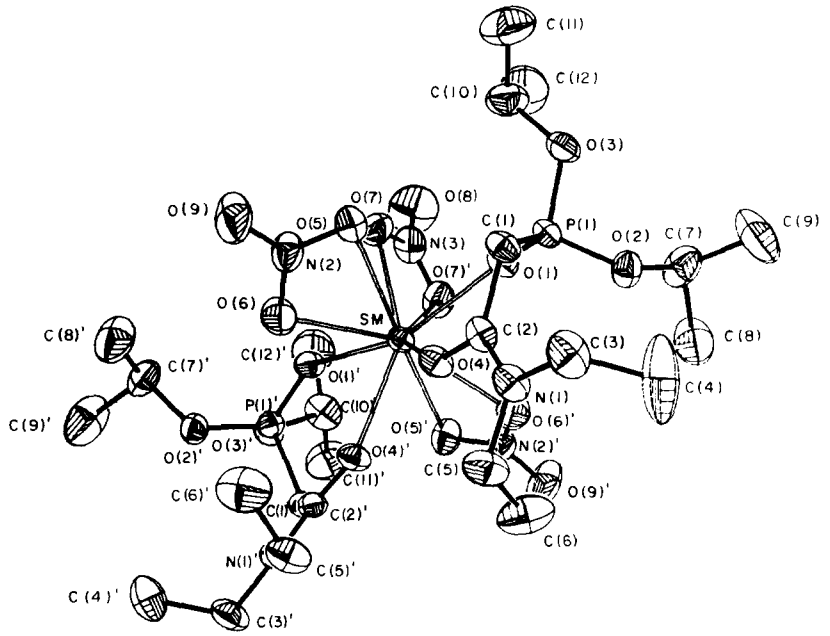

Fig. 1. Molecular geometry and labeling scheme for $Sm[(i\text{-}C_3H_7O)_2P(O)CH_2C(O)N(C_2H_5)_2]_2(NO_3)_3$ (50% probability ellipsoids).

The single crystal X-ray analyses of *3* and *4* indicate that the correct formulations are $Sm[(i\text{-}C_3H_7O)_2P(O)CH_2C(O)N(C_2H_5)_2]_2(NO_3)_3$ and $Er[(i\text{-}C_3H_7O)_2P(O)CH_2C(O)N(C_2H_5)_2]_2(NO_3)_3 \cdot H_2O$, respectively. The structure of *3* contains discrete monomeric units having C_2 symmetry with four molecules in the unit cell. A view of the molecular unit is shown in Fig. 1. Selected interatomic distances and angles are summarized in Tables IV and V.

The central samarium atom is bonded to two bidentate, neutral DiPDECMP ligands and three bidentate nitrate ions which provide a total coordination number of ten. The samarium–phosphoryl oxygen atom bond distance, Sm–O(1) 2.418(3) Å, is slightly longer than the samarium–phosphoryl oxygen atom distances in the seven coordinate complex $[Sm(S_2P(OEt)_2)_2(P(O)Ph_3)_3^+][(S_2P(OEt)_2^-]$, 2.30(1), 2.32(1) and 2.28(2) Å [21]. Comparative data for related ten coordinate Sm(III) complexes do not appear to be available. Consequently, a comparison of the M–O (phosphoryl) bond distances in *3* and the Th(IV) complex, *2*, is warranted [12]. Although the metal atom coordination numbers and effective ionic radii [22] differ in these complexes, the bond distances, Sm–O(1) 2.418(3) Å and Th–O(1) 2.482(4) Å, suggest that the samarium–phosphoryl oxygen atom interaction, corrected for metal ionic radius differences, is shorter by approximately 0.11 Å. The samarium–carbonyl oxygen bond distance, Sm–O(4) 2.433(2) Å, is similar to reported samarium–oxygen atom bond distances in several carboxylate complexes, $[Sm_2(C_5H_4NCO_2)_6 \cdot (H_2O)_4]$ 2.360(3)–2.565(3) Å [23] and $Sm(C_7H_5O_3)_3 \cdot H_2O$

TABLE V. Selected Interatomic Angles (°) Sm(DiPDECMP)$_2$(NO$_3$)$_3$.

O(1)–Sm–O(4)	73.9(1)
O(5)–Sm–O(6)	48.1(1)
O(7)–Sm–O(7')	50.1(2)
O(5)–Sm–O(1)	72.8(1)
O(6)–Sm–O(1)	120.5(1)
O(5)–Sm–O(4)	69.6(1)
O(6)–Sm–O(4)	79.1(1)
O(5)–Sm–O(7)	64.0(1)
O(6)–Sm–O(7)	84.7(2)
O(5)–Sm–O(7')	111.9(1)
O(6)–Sm–O(7')	128.5(2)
O(1)–Sm–O(1)	145.4(1)
Sm–O(4)–C(2)	141.0(2)
Sm–O(1)–P(1)	135.5(2)
O(1)–P(1)–O(2)	116.4(2)
O(1)–P(1)–O(3)	112.6(1)
O(2)–P(1)–O(3)	104.8(2)
O(1)–P(1)–C(1)	113.1(2)
O(2)–P(1)–C(1)	101.9(2)
O(3)–P(1)–C(1)	107.1(2)
O(4)–C(2)–C(1)	118.0(3)
N(1)–C(2)–O(4)	120.8(3)
N(1)–C(2)–C(1)	121.2(2)
P(1)–C(1)–C(2)	110.4(3)
O(5)–N(2)–O(6)	116.4(5)
O(5)–N(2)–O(9)	122.3(4)
O(6)–N(2)–O(9)	121.3(5)
O(7)–N(3)–O(8)	121.9(3)
O(7)–N(3)–O(7')	116.1(5)

2.371(4)–2.588(3) Å [24]. Comparison of M–O (carbonyl) distances in *2*, 2.453(4) Å, and *3* corrected for ionic radii differences shows that these effective bond distances are more nearly alike (~0.04 Å difference).

There are two non-equivalent sets of nitrate groups in *3*. $N(3)O_3$ lies on the C_2 rotation axis, and it is unique. $N(2)O_3$ and $N(2')O_3$ are related by the C_2 rotation axis. $N(3)O_3$ occupies a symmetrical bidentate coordination position with Sm–O(7) 2.518(4) Å. $N(2)O_3$ and $N(2')O_3$ are asymmetrically bonded to the Sm(III) atom as indicated by the difference in the Sm–O(5) and Sm–O(6) distances, 2.731(4) Å and 2.518(5) Å. These distances are similar to distances found in a number of lanthanide bidentate nitrate complexes: $Yb[(CH_3)_2SO]_3(NO_3)_3$ $Yb–O(nitrate)_{avg}$ 2.43(4) Å [25], $La[(CH_3)_2SO]_3(NO_3)_3$ $La–O(nitrate)_{avg}$ 2.65(3) Å [26].

The coordination polyhedron in *3* roughly approximates a bicapped square antiprism with the oxygen atoms of each DiPDECMP ligand spanning adjacent coordination positions on one square plane edge. Decacoordination polyhedra have been observed for $La(NO_3)_3(bipyridine)_2$ [27] and $La[(CH_3)_2SO]_4(NO_3)_3$ [28]. A view of the polyhedron is shown in Fig. 2 and a listing of selected nonbonded oxygen atom–oxygen atom distances is given in Table S-3 [18]. These distances range from 2.132(7) Å to 3.393(5) Å with the three shortest distances corresponding to the 'bite' distances of the three bidentate nitrate ions. These distances are shorter than the sum of the ionic radii for oxide ion, 2.8 Å, and this short distance may be partially responsible for stabilizing the ten coordinate structure.

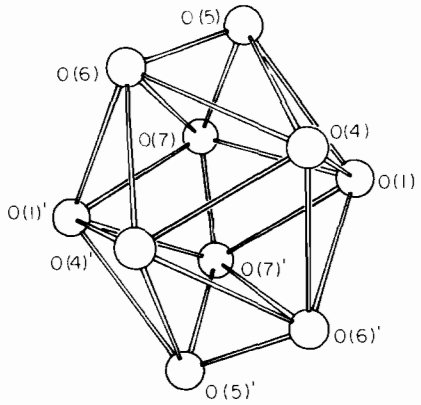

Fig. 2. Representation of the oxygen atom coordination polyhedron about the samarium atom.

The structure of *4* contains discrete monomeric units with two molecules per unit cell. A view of the molecular unit is shown in Fig. 3. Selected interatomic distances and angles are summarized in Tables VI and VII. Unlike *2* and *3*, the central erbium atom is bonded to two inequivalent monodentate, neutral

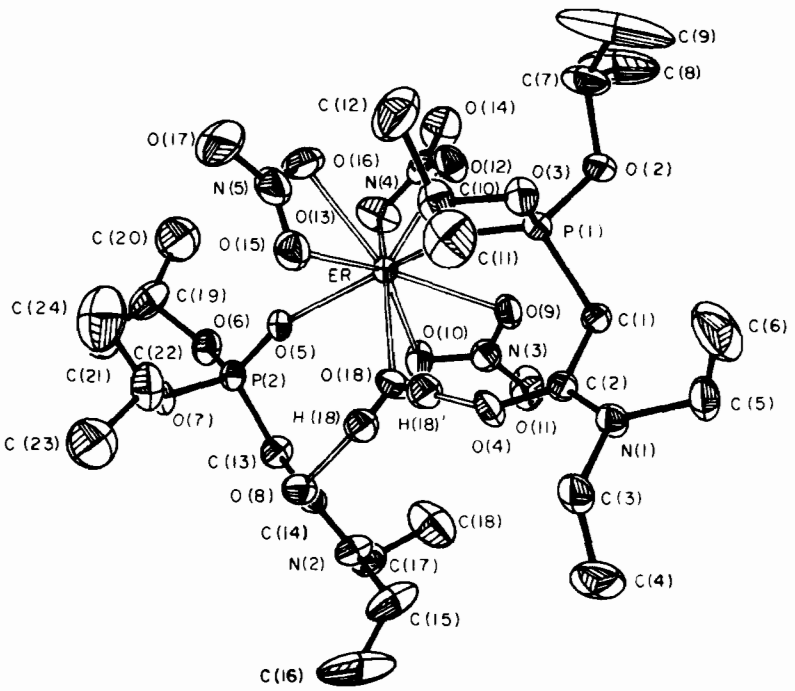

Fig. 3. Molecular geometry and labeling scheme for $Er[(i\text{-}C_3H_7O)_2P(O)CH_2C(O)N(C_2H_5)_2]_2(NO_3)_3 \cdot H_2O$ (50% probability ellipsoids). Atom O(1) is underneath atom C(11).

TABLE VI. Selected Interatomic Distances (Å) for Er(DiPDECMP)$_2$(NO$_3$)$_3$·H$_2$O.

Er–O(1)	2.259(6)	Er–O(13)	2.406(9)
Er–O(5)	2.290(6)	Er–O(15)	2.467(7)
Er–O(9)	2.451(7)	Er–O(16)	2.401(8)
Er–O(10)	2.460(7)	Er–O(18)	2.302(7)
Er–O(12)	2.422(8)	P(2)–O(5)	1.452(7)
P(1)–O(1)	1.479(6)	P(2)–O(6)	1.556(7)
P(1)–O(2)	1.544(7)	P(2)–O(7)	1.544(7)
P(1)–O(3)	1.561(6)	P(2)–C(13)	1.794(10)
P(1)–C(1)	1.789(8)	C(13)–C(14)	1.504(14)
C(1)–C(2)	1.518(11)	C(14)–O(8)	1.240(11)
C(2)–O(4)	1.239(11)	C(14)–N(2)	1.313(13)
C(2)–N(1)	1.340(11)	N(2)–C(15)	1.495(19)
N(1)–C(3)	1.481(12)	N(2)–C(17)	1.511(14)
N(1)–C(5)	1.447(14)	*C(15)–C(16)	1.35(5)
C(3)–C(4)	1.509(18)	C(17)–C(18)	1.48(2)
C(5)–C(6)	1.493(19)	O(6)–C(19)	1.455(14)
O(2)–C(7)	1.485(14)	O(7)–C(22)	1.462(14)
O(3)–C(10)	1.464(12)	*C(19)–C(20)	1.47(4)
C(7)–C(8)	1.43(2)	*C(19)–C(21)	1.53(4)
C(7)–C(9)	1.32(3)	*C(22)–C(23)	1.59(5)
C(10)–C(11)	1.48(2)	C(22)–C(24)	1.42(2)
C(10)–C(12)	1.48(2)	N(4)–O(12)	1.249(13)
N(3)–O(9)	1.265(12)	N(4)–O(13)	1.241(14)
N(3)–(10)	1.251(12)	N(4)–O(14)	1.209(12)
N(3)–O(11)	1.216(12)	O(18)–H(181)	0.78(9)
N(5)–O(15)	1.215(15)	O(18)–H(182)	0.76(9)
N(5)–O(16)	1.251(16)	O(4)–H(182)	1.88(9)
N(5)–O(17)	1.248(16)	O(8)–H(181)	1.96(9)

*Average distances for disordered positions.

DiPDECMP ligands. In addition, the metal atom is bonded to three bidentate nitrate ions and the oxygen atom of a water molecule, and the total coordination number is nine. The DiPDECMP–Er coordination occurs only through the phosphoryl oxygen atoms, and the interatomic distances are surprisingly different. Er–O(1) 2.259(6) Å and Er–O(5) 2.290(6) Å. Taking into account differences in ionic radii [22], these bond distances are both significantly shorter than the metal–phosphoryl oxygen atom distances in the bidentate CMP complexes *2* and *3*. On the other hand, the erbium–carbonyl oxygen atom interatomic distances, Er···O(4) and Er···O(8), are greater than 4.0 Å, and they are considered to be nonbonding separations. The erbium–water oxygen distance, Er–O(18) 2.302(7) Å, is similar to coordinated water distances in Er$_2$(C$_2$O$_2$H$_3$)$_6$·4H$_2$O [29] 2.30(3)–2.31(3) Å, and [Er(HOCH$_2$COO)(OCH$_2$COO)(H$_2$O)]·H$_2$O [30] 2.34(1) Å. The water hydrogen atoms were located and the interatomic distances O(18)–H(181) 0.78(9) Å, O(18)–H(182) 0.76(9) Å, O(4)···H(182) 1.88(9) Å, O(8)···H(181) 1.96(9) Å, O(8)···O(18) 2.711(9) Å and O(4)···O(18) 2.634(9) Å are consistent with hydrogen bonding interactions between the two

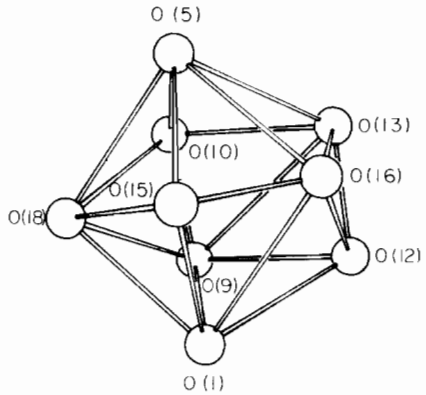

Fig. 4. Representation of the oxygen atom coordination polyhedron about the erbium atom.

carbonyl oxygen atoms and the coordinated water molecule. The erbium–O(nitrate) bond distances range from 2.401(8) Å to 2.467(7) Å, and these distances are similar to those reported for bidentate nitrate groups in Er[(CH$_3$)$_2$SO]$_3$(NO$_3$)$_3$ 2.39(3)–2.54(2) Å [30].

The coordination polyhedron for *4* approximates a tricapped trigonal prism with the phosphoryl oxygen atom O(1) occupying a position on one trigonal base while the second phosphoryl oxygen atom O(5) occupies a position on the second trigonal base. A similar polyhedron has been reported for the complex Er[(CH$_3$)$_2$SO]$_4$(NO$_3$)$_3$ [30]. A view of the polyhedron is shown in Fig. 4 and a listing of selected nonbonding oxygen atom–oxygen atom distances is available (Table S–3) [18]. These distances range from 2.09(1) Å to 3.31(1) Å with the three shortest distances corresponding to the 'bite' distances in the bidentate nitrate groups.

Several structural features of the coordinated CMP ligands and the nitrate groups are notable. The DiPDECMP ligands clearly exist in the neutral form and the phosphorus atom environments are tetrahedral. The phosphoryl group, P–O, distances, *3*, 1.480(2) Å and *4* 1.479(6) and 1.452(7) Å compare favorably with distances found in *1* 1.45(1) Å [11] and *2* 1.478(4) Å [12]. The carbonyl distance in *3*, C(2)–O(4) 1.261(3) Å compares favorably with the corresponding distance in *2*, 1.256(6) Å. In both complexes, the CMP ligand is bonded to a central metal atom in a bidentate fashion. The carbonyl distances in *4*, C(2)–O(4) 1.239(11) Å and C(14)–O(8) 1.240(11) Å, are slightly shorter than the carbonyl distance in *3* and similar to the carbonyl distance in *1*, 1.24(2) Å. The large standard deviations on these distances make comparisons difficult; however, the trend in carbonyl bond shortening in *4* is consistent with the absence of metal ion coordination and the presence of weaker hydrogen bond interactions. In addition, the shorter distance Er–O(1) and longer distance O(1)–P(1) within one

TABLE VII. Selected Interatomic Angles (°) for $Er(DiPDECMP)_2(NO_3)_3 \cdot H_2O$.

O(1)–Er–O(5)	148.1(2)	O(1)–Er–O(9)	75.4(2)
O(5)–Er–O(10)	72.9(2)	O(9)–Er–O(10)	51.3(2)
O(1)–Er–O(12)	75.7(2)	O(5)–Er–O(13)	82.3(3)
O(12)–Er–O(13)	51.3(3)	O(10)–Er–O(13)	72.6(3)
O(5)–Er–O(16)	83.7(3)	O(1)–Er–O(15)	75.3(2)
O(1)–Er–O(18)	77.7(2)	O(9)–Er–O(16)	146.6(3)
O(15)–Er–O(18)	75.4(3)	O(12)–Er–O(16)	74.2(3)
O(10)–Er–O(18)	76.6(2)	O(15)–Er–O(16)	52.0(3)
O(13)–Er–O(18)	148.1(3)	O(5)–Er–O(18)	81.1(2)
Er–O(1)–P(1)	159.6(3)	Er–O(5)–P(2)	161.7(4)
O(1)–P(1)–O(2)	114.8(4)	O(5)–P(2)–O(6)	115.2(4)
O(2)–P(1)–O(3)	106.8(3)	O(6)–P(2)–O(7)	104.5(4)
O(2)–P(1)–C(1)	100.5(4)	O(6)–P(2)–C(13)	98.3(4)
O(1)–P(1)–O(3)	112.0(3)	O(5)–P(2)–O(7)	113.8(4)
O(1)–P(1)–C(1)	114.3(4)	O(5)–P(2)–C(13)	114.0(4)
O(3)–P(1)–C(1)	107.5(4)	O(7)–P(2)–C(13)	109.5(5)
P(1)–C(1)–C(2)	112.8(5)	P(2)–C(13)–C(14)	114.0(6)
O(4)–C(2)–C(1)	119.1(8)	O(8)–C(14)–N(2)	123.2(9)
O(4)–C(2)–N(1)	121.4(7)	O(8)–C(14)–C(13)	119.4(8)
O(4)–C(2)–C(1)	119.1(8)	N(2)–C(14)–C(13)	117.4(8)
N(1)–C(2)–C(1)	119.4(8)	O(12)–N(4)–O(13)	114.2(8)
O(9)–N(3)–O(10)	115.3(8)	O(13)–N(4)–O(14)	123.2(11)
O(10)–N(3)–O(11)	124.0(10)	O(12)–N(4)–O(14)	122.6(11)
O(9)–N(3)–O(11)	120.7(10)	H(181)–O(18)–H(182)	112(9)
O(15)–N(5)–O(16)	119.9(10)		
O(16)–N(5)–O(17)	116.8(12)		
O(15)–N(5)–O(17)	123.2(12)		

CMP–Er interaction suggests that this ligand may be more tightly bonded to the Er ion than the second CMP ligand. The P–O(i-Pr) and P–C(methylene) bond distances and the bond angles about the phosphoryl P atoms and carbonyl C atoms in *3* and *4* are also similar to the respective parameters in *2*.

The nitrate groups in *3* and *4* are planar and the ranges of N–O bond distances, *3* 1.212(8) to 1.279(4) Å and *4* 1.209(12) to 1.265(12) Å are similar to distances observed for *2*. In *3*, the N–O bond distances involving the coordinated oxygen atoms are longer than the N–O bond distance for the uncoordinated oxygen atom. In addition, the N–O distances, N(2)–O(5) 1.248(7) and N(2)–O(6) 1.279(4) are significantly different and the asymmetry is clearly associated with the shorter Sm–O(6) distance compared with Sm–O(5). In *4*, the NO_3^- groups containing N(3) and N(4) appear to be normal symmetric bidentate nitrate ligands; the N–O bond containing the uncoordinated oxygen atoms is shorter than the N–O bonds containing the coordinated oxygen atoms. The NO_3^- group containing N(5) is unique. The N–O bond distances involving the coordinated oxygen atoms are surprisingly asymmetric, N(5)–O(15) 1.215(15) Å and N(5)–O(16) 1.251(16) Å, and the uncoordinated N–O bond distance, N(5)–O(17) 1.248(16) Å is unusually long. This asymmetry appears to be unique in structures containing bidentate nitrate–metal ion interactions. A simple explanation for this structural distortion is not obvious. However, it is intriguing to consider that a nonbonded lone pair (water oxygen atom O(18)–O(15)) interaction may be operating. Such an interaction might be expected to weaken the Er–O(15) interaction. Indeed, that bond distance is the longest of the Er–oxygen atom interatomic distances. A weakening in the Er–O(15) interaction in turn would result in a shorter N(5)–O(15) bond distance.

The solid state structures for *3* and *4* contain unique features which could not be predicted from the solution phase spectroscopic data. In particular, the monodentate phosphoryl–metal atom bonding of the CMP ligands in *4* was not clearly indicated by the infrared data. The down-frequency ν_{CO} shift in *4* as compared to ν_{CO} in the free ligand was initially interpreted to indicate bidentate CMP coordination; however, this shift must occur in response to the carbonyl oxygen–hydrogen bond interaction clearly observed in the X-ray structure. These results indicate that great care must be exercised in deducing solution state structures in these complexes from infrared spectroscopic data alone. Additional studies on related complexes are in progress.

Acknowledgements

RTP wishes to acknowledge the financial support for this work from the Department of Energy, Office of Basic Energy Sciences, Grant No. 79ER-10465. We also wish to recognize the NSF Grant CHE-7802921 which facilitated the purchase of the X-ray diffractometer and the NSF Grant CHE-8007979 which facilitated the purchase of the Fourier transform infrared spectrometer.

References

1 W. W. Schulz and L. D. McIsaac, 'Transplutonium Elements', W. Müller and R. Lindmer, Ed., North Holland, Amsterdam (1976), p. 433.
2 T. H. Siddall, *J. Inorg. Nucl. Chem., 25,* 883 (1963).
3 T. H. Siddall, *J. Inorg. Nucl. Chem., 26,* 1991 (1964).
4 W. W. Schulz, Rept. ARH-SA-203, Atlantic Richfield Co., Hanford WA., (1974).
5 L. D. McIsaac, J. D. Baker, J. F. Krupa, R. E. LaPointe, D. H. Meikrantz and N. C. Schroeder, Rept. ICP-1180, Allied Chemical Co., Idaho Chemical Programs, Idaho Falls, ID, (1979).
6 L. D. McIsaac, J. D. Baker, J. F. Krupa, D. H. Meikrantz and N. C. Schroeder, 'Actinide Separations', ACS Symposium Ser., *117, 395 (1980).*
7 H. Petrzilova, J. Binca and L. Kuca, *J. Radioanal. Chem., 51,* 107 (1979).
8 W. E. Stewart and T. H. Siddall, *J. Inorg. Nucl. Chem., 32,* 3599 (1970).
9 D. G. Kalina, E. P. Horwitz, L. Kaplan and A. C. Muscatello, *Sep. Sci. Tech.,* submitted.
10 E. P. Horwitz, A. C. Muscatello, D. G. Kalina and L. Kaplan, *Sep. Sci. Tech., 16,* 417 (1981).
11 S. M. Bowen, E. N. Duesler, R. T. Paine and C. F. Campana, *Inorg. Chim. Acta, 59,* 53 (1982).
12 S. M. Bowen, E. N. Duesler and R. T. Paine, *Inorg. Chem., 21,* 261 (1982).
13 Similar reactions were performed with La, Pr, Nd, Eu, Gd, and Dy nitrates and products identical to those reported previously were obtained [8]. The full characterization of these complexes will be reported separately.
14 The P3/F and R3 hardware configuration has been described: C. F. Campana, D. F. Sheppard and W. N. Litchman, *Inorg. Chem., 19,* 4039 (1981). Crystal centering, autoindexing, cell parameter refinement and axial photograph programs are those described in the 'Nicolet P3/R3 Operations Manual', Nicolet XRD Corp. 1980. All calculations and plots were performed with the SHELXTL–79 package, G. M. Sheldrick, 'Nicolet SHELXTL Operations Manual', 1979. SHELXTL uses scattering factors compiled in 'International Tables for X-ray Crystallography', Vol. IV , Kynock Press, Birmingham, U.K. (1968).
15 A general description of the least squares algebra is found in 'Crystallographic Computing', F. R. Ahmed, S. R. Hall and C. P Huber, Ed., Munksgaard, Copenhagen (1970) p. 187.
16 All Fourier calculations required that $\sin\theta \leqslant 0.57$ in order that storage requirements not be exceeded.
17 $F = F_o[1 - (x|F_o|^2 \cdot 10^{-4})/\sin\theta]$.
18 Supplementary data.
19 The doublet structure in the ν_{CO} band in *3* was initially interpreted in favor of the presence of metal bonded and nonbonded carbonyl groups [3]. However, the lack of similar structure in benzene solution was used to reject this interpretation [3]. A detailed study of solution infrared spectra as a function of solvents is in progress in our laboratory.
20 The influence of paramagnetic shift reagents on carbonyl and phosphoryl groups has been studied by ^{31}P and ^{13}C NMR spectroscopy: C. M. Dobson, R. J. P. Williams and A. V. Xavier, *J. Chem. Soc. (Dalton Trans.),* 2662 (1973);
J. K. M. Sanders and D. H. Williams, *Tet. Lett., 30,* 2813 (1971);
G. N. LaMar, W. D. Horrocks, Jr. and R. H. Holm, Ed., 'Chemical Applications of NMR in Paramagnetic Molecules', Academic Press, New York, N.Y., 1973.
21 A. A. Pinkerton and D. Schwarzenbach, *J. Chem. Soc. (Dalton Trans.),* 2466 (1976).
22 R. D. Shannon and C. T. Prewitt, *Acta Crystallogr., B25,* 925 (1969). The effective ionic radii with coordination number of eight were used in our comparisons; Th(IV) 1.06 Å, Sm(III) 1.09 Å, Er(III) 1.00 Å.
23 J. W. Moore, M. D. Glick and W. A. Baker, Jr., *J. Am. Chem. Soc., 94,* 1858 (1972).
24 J. H. Burns and W. H. Baldwin, *Inorg. Chem., 16,* 289 (1977).
25 K. K. Bhandary, H. Manohar and K. Venkatesan, *J. Chem. Soc. (Dalton Trans.),* 288 (1975).
26 K. K. Bhandary, H. Manohar and K. Venkatesan, *J. Inorg. Nucl. Chem., 37,* 1997 (1975).
27 A. R. Al-Karaghouli and J. S. Wood, *J. Am. Chem. Soc., 90,* 6548 (1968).
28 K. K. Bhandary and H. Manohar, *Acta Crystallogr., B29,* 1093 (1973).
29 L. A. Aslanov, I. K. Abdul'minev, M. A. Porai-Koshits and I. V. Ivanov, *Dokl. Akad. Nauk. USSR, 205,* 343 (1972).
30 I. Grenthe, *Acta Chem. Scand., 23,* 1253 (1969).
31 L. A. Aslanov, L. I. Soleva and M. A. Porai-Koshits, *Zh. Struk. Khim., 13,* 1101 (1972).